For Flow cytometry			
Antibody Target	**Dilution**	**Clone**	**Supplier**
mCD3	1:200	17A2	BD Bioscience
mCD4	1:200	GK1.5	Invitrogen
mCD8	1:200	53-6.7	Biolegend
mCD11b	1:200	M1/70	Biolegend
mCD11c	1:200	N418	Biolegend
mCD19	1:200	115508	Biolegend
mCD25	1:200	PC61.5	eBioscience
mCD45	1:200	30-F11	Biolegend
mCD64	1:200	X54-5/7.1	Biolegend
mF4/80	1:200	BM8	Biolegend
mFOXP3	1:200	MF-14	Biolegend
mLy6C	1:200	HK1.4	Biolegend
mLy6G	1:200	1A8	BD Bioscience
MHCII I-A/I-E	1:200	M5/114.15.2	Biolegend
mCCR2	1:200	FAB5538A	R&D Systems
mTim4	1:200	F31-5G3	Biolegend
mVegf-C	1:200	E-6	SCBT
Zombie Aqua Fixable Viability Kit	1:1000	Cat#: 423101	Biolegend
For Immunofluorescence/Western Blotting			
Antibody Target	**Dilution**	**Clone/Catalog #**	**Supplier**
Goat anti-mouse IgG A594	1:500	Poly4053	Biolegend
Goat anti-mouse IgG A488	1:500	Poly4053	Biolegend
Donkey anti-goat TR	1:500	SAB3700320	MilliporeSigma
Anti-Lyve1	1:200	BAF2125	R&D Systems
CD68	1:200	FA-11	Biolegend
PECAM	1:1000	553370	Pharmingen
pStat6	1:1000	Cat#: mab56554	Cell Signaling
Stat6	1:1000	mab5397	Cell Signaling
Beta Actin-HRP	1:1000	2F1-1	Biolegend
Chemicals/Recombinant Proteins/Commercial Kits			
RNAeasy Plus mini kit	Cat#: 74034		Qiagen
TruSeq® Stranded mRNA Library Prep	Cat#: 20020594		Illumina
Anti-Histone H3 (acetyl K27)	ab4729		Abcam
Mouse Vegfc ELISA Kit	Cat#: CSB-E07361m		Cusabio
Cytochlasin D	Cat#: C8273-1MG		MilliporeSigma
Etomoxir	Cat#: E1905		MilliporeSigma
Lipopolysaccharide from E. coli O111:B4	Cat#: L4391		MilliporeSigma
RBC Lysis Buffer (10X)	Cat#: 420301		BioLegend
Neomycin solution	Cat#: N1142		MilliporeSigma
2,3,5-Triphenyltetrazolium chloride	Cat#: T8877		MilliporeSigma
MAZ51	Cat#: 06-127		MilliporeSigma
Sirius Red (Direct Red 80)	Cat#: 365548-5G		MilliporeSigma
FluoroSpheres (580/605)	Cat#: F8834		ThermoScientific
Collagenase Type 2	Cat#: LS004177		Worthington

Supplemental Table I.

Primer Lists	
Target	**Sequence**
Vegf-c	Vegfc-F: TCC CCT GTC CTG GTA TTG AG Vegfc-R: CGA GGT CAA GGC TTT TGA AG
Tnf alpha	Tnf-F: ACG GCA TGG ATC TCA AAG AC Tnf-R: AGA TAG CAA ATC GGC TGA CG
IL1Beta	Il1b-F: TAC GGA CCC CAA AAG ATG A Il1b-R: TGC TGC TGC GAG ATT TGA AG
IL6	Il6-F: GCC TTC TTG GGA CTG ATG CT Il6-R: TGC CAT TGC ACA ACT CTT TTC
IL12	mIL12-F: ACGAGAGTTGCCTGGCTACTAG mIL12-R: CCTCATAGATGCTACCAAGGCAC
Arg1	Arg1-F: ATGGAAGAGACCTTCAGCTAC Arg1-R: GCTTTCCCAACAGTTGGG
B2M	B2m-F: CTG CTA CGT AAC ACA GTT CCA CCC B2m-R: CAT GAT GCT TGA TCA CAT GTC TCG

Supplemental Table II.

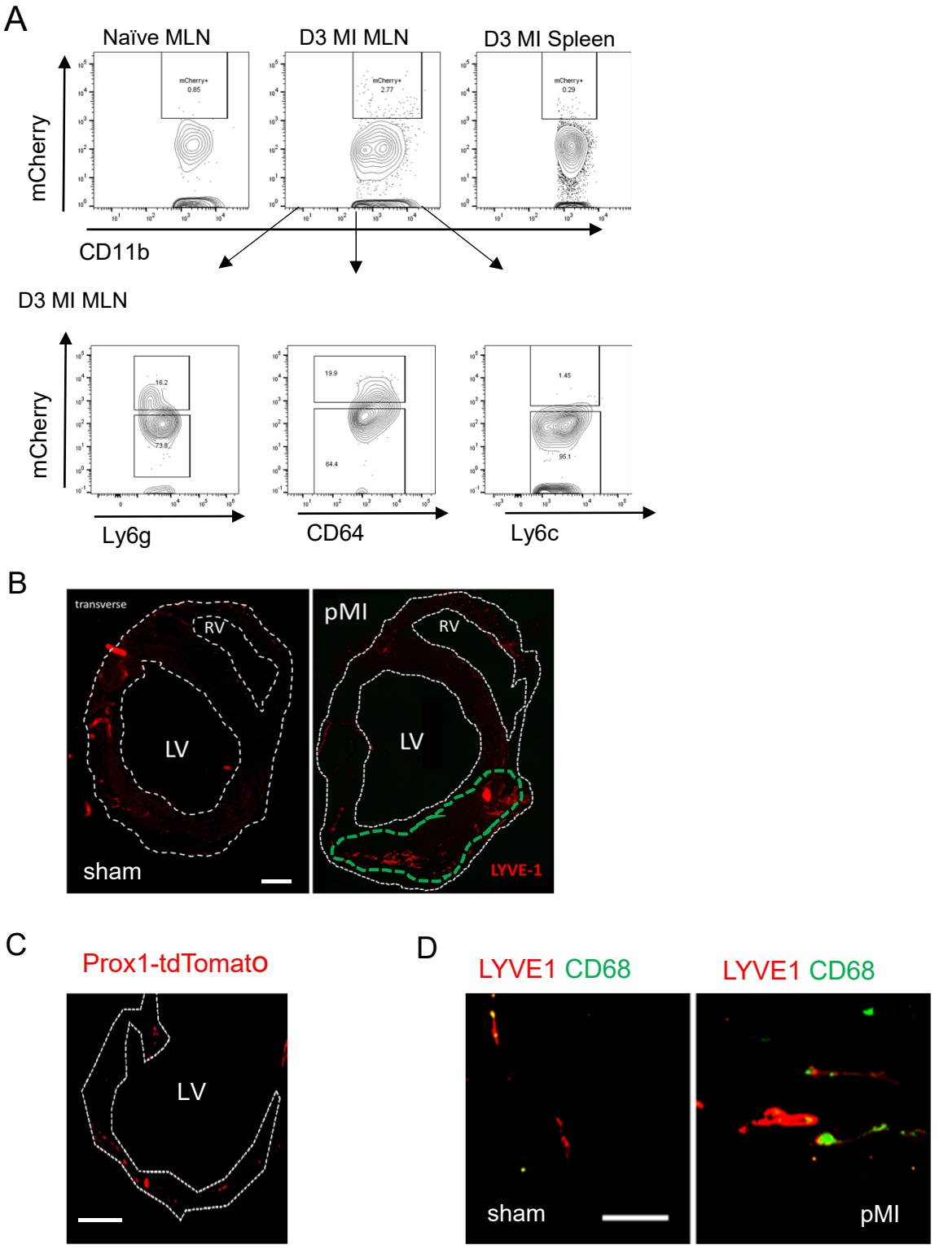

Supplemental Figure 1. Experimental myocardial infarction (MI) induces markers of cardiac lymphangiogenesis. (**A**) Representative flow cytometric analysis of MLNs from mCherry mice prior to and post LAD ligation. Top panel shows mCherry antigen uptake by CD11b+ cells in mediastinal lymph nodes and spleen 3 days post MI. Bottom panel shows mCherry antigen uptake 3 days post MI by Ly6g^{+} neutrophils, CD64^{+} F4/80^{+} macrophages and Ly6c^{hi} monocytes. (**B**) Left anterior descending (LAD) arteries of C57BL/6J adult mice were ligated and transverse cross sections stained by fluorescent immunohistochemistry for LYVE1 (lymphatic vessel endothelial receptor 1) tubular staining post MI (pMI) versus sham surgery control. White dotted lines circumscribe the heart and LV indicates left ventricle while RV indicates right ventricle. Green-dotted line indicates ischemic area at risk. Images taken of hearts at ~7 days post MI. (Scale bar = 1mm) (**C**) Prox1-tdTomato mice were subjected to ligation of the LAD and *Prox1Tdtomato* images acquired at the circumscribed infarct area at risk by fluorescent microscopy. (Scale bar = 1mm) (**D**) Tubular LYVE1+ CD68-negative tubular staining in C57BL/6J sham mice versus LAD-ligated mice. (Scale bar = 100μm).

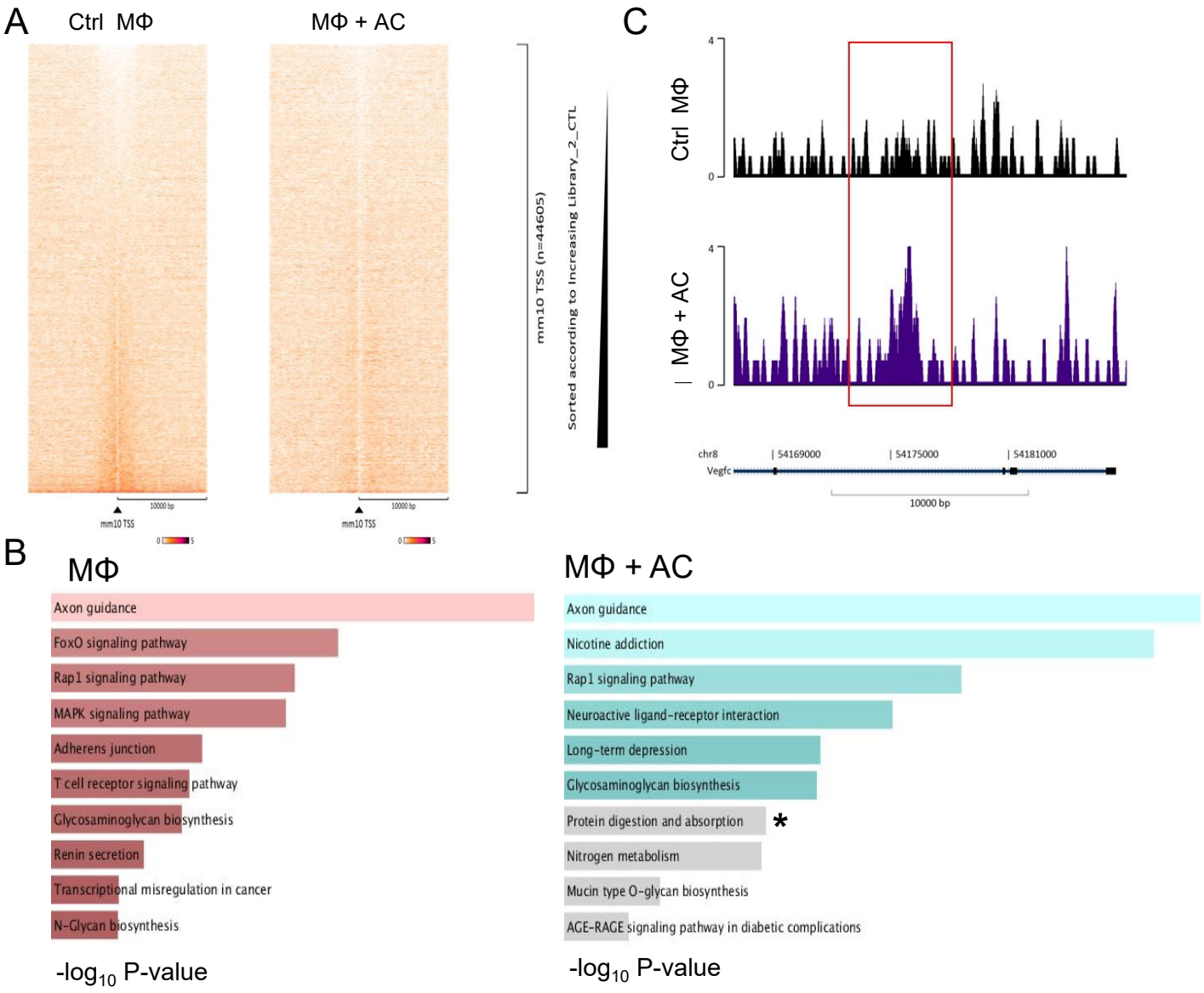

D

footprintDB template	Source	Organisms	STAMP e-value	Motif similarity	footprinDB PWM / Consensus
PB0166.1: Sox12_2	JASPAR 2016	Mus musculus	2.5e-04	6.60 / 10	-----tTkCTcwMwG- awtyCTTTGTstrwkk
M0310_1.02: Cebpe / T025966_1.02	CISBP 1.02	Mus musculus	6.5e-04	5.30 / 8	tTkCTcwMwG TTwyGCAA--
MA0520.1: Stat6	JASPAR 2016	Mus musculus	7.4e-04	6.33 / 10	-tTkCTcwMwG---- rkTTCtswrGAArws

Supplemental Figure 2. Epigenetic screen for open chromatin accessibility mark Histone3K27Acetylation (H3K27Ac) after efferocytosis implicates transcriptional activation of *Vegfc* and open transcription factor binding site footprints. Primary macrophages were cultured without (Ctrl) versus with apoptotic cells (AC) and subjected to chromatin immunoprecipitation sequencing (ChIP-seq) for H3K27ac. **(A)** Mus musculus (mm10) genome assembly heatmap of H3K27ac ChIP-seq signal at transcription start sites (TSS) across the mouse genome. Analyzed with University of California Santa Cruz Genome Browser. (**B**) KEGG pathway analysis of genes associated with the top 3000 peak score regions. Notable enrichment for “protein digestion and absorption” in apoptotic cells-treat group. (**C**) Evidence of increased chromatin accessibility at sites within the *Vegfc* locus. (**D**) Transcription factor footprint analysis at open chromatin sites during efferocytosis.

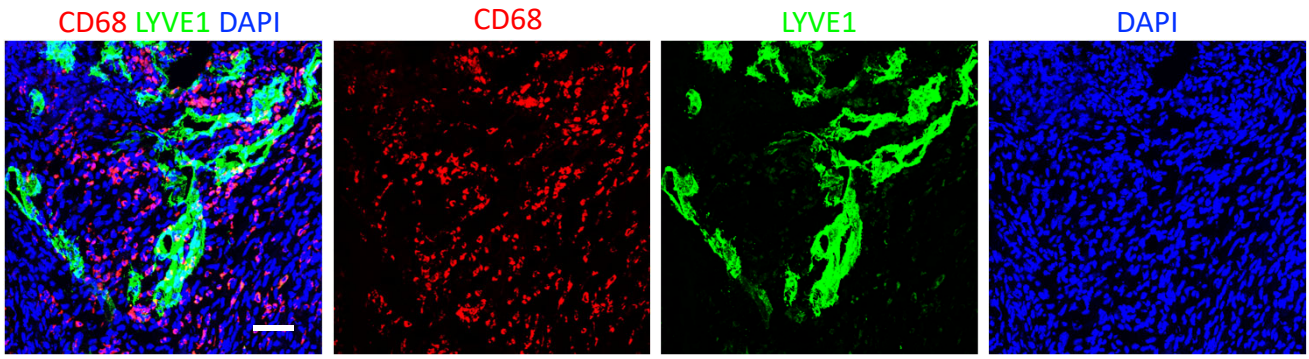

Supplemental Figure 3. Juxtaposition of cardiac CD68 positive macrophage cells with LYVE1 lymphatic cells. LYVE1+ lymphatic endothelial cell (LEC) cells are stained green, and $CD68^{+}$ macrophage cells are stained red. Images were taken from cardiac sections after coronary artery ligation of experimental mice at ~1week post MI. Scale bar = 50μm.

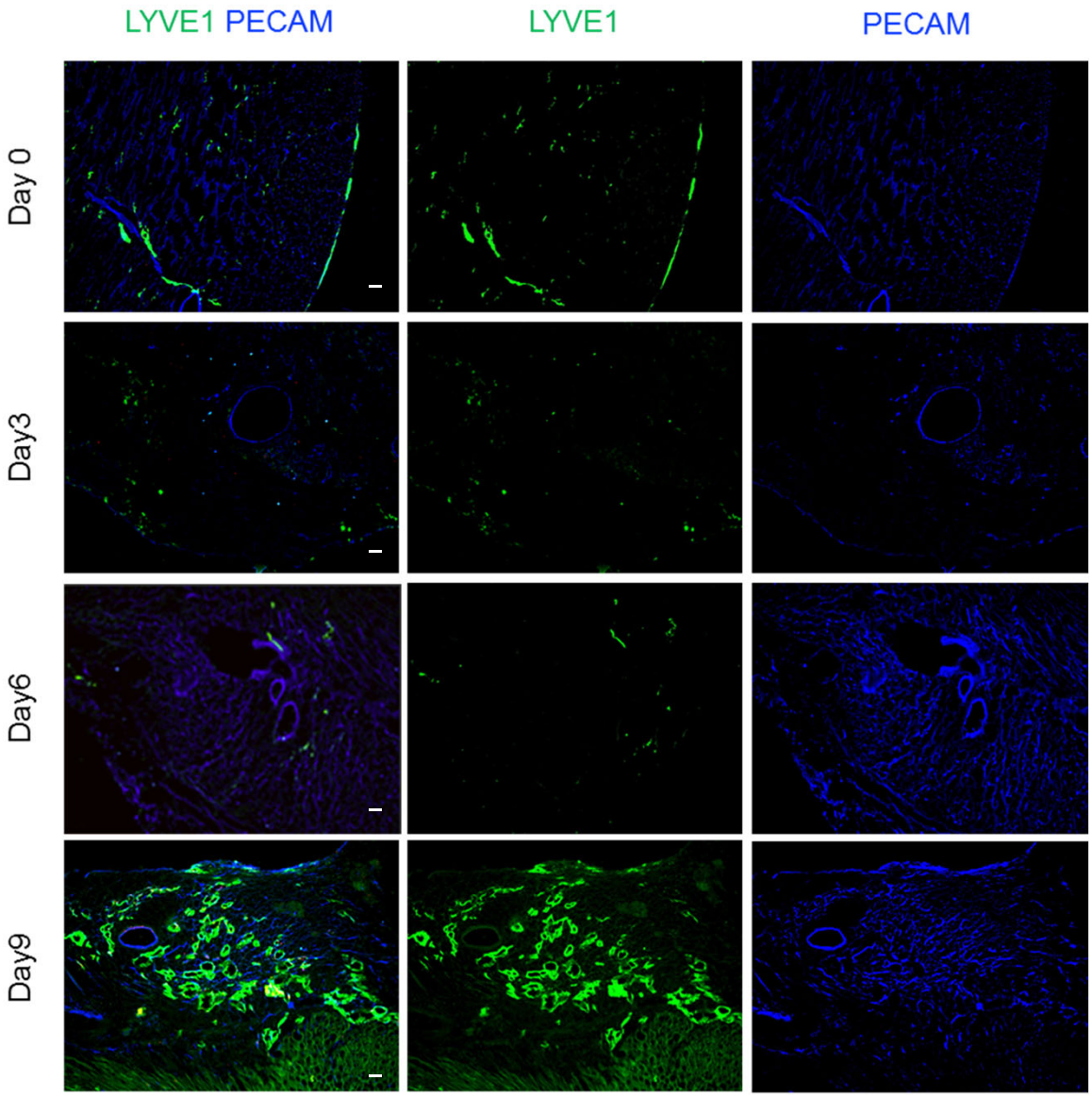

Supplemental Figure 4. Time course of LYVE1 staining after ischemia then reperfusion (I/R) in mice. Myocardial Immuno-fluorescent staining of indicated markers in transverse cross-sections of mice after cardiac I/R. Times are days post I/R. Scale bar = 50 μm.

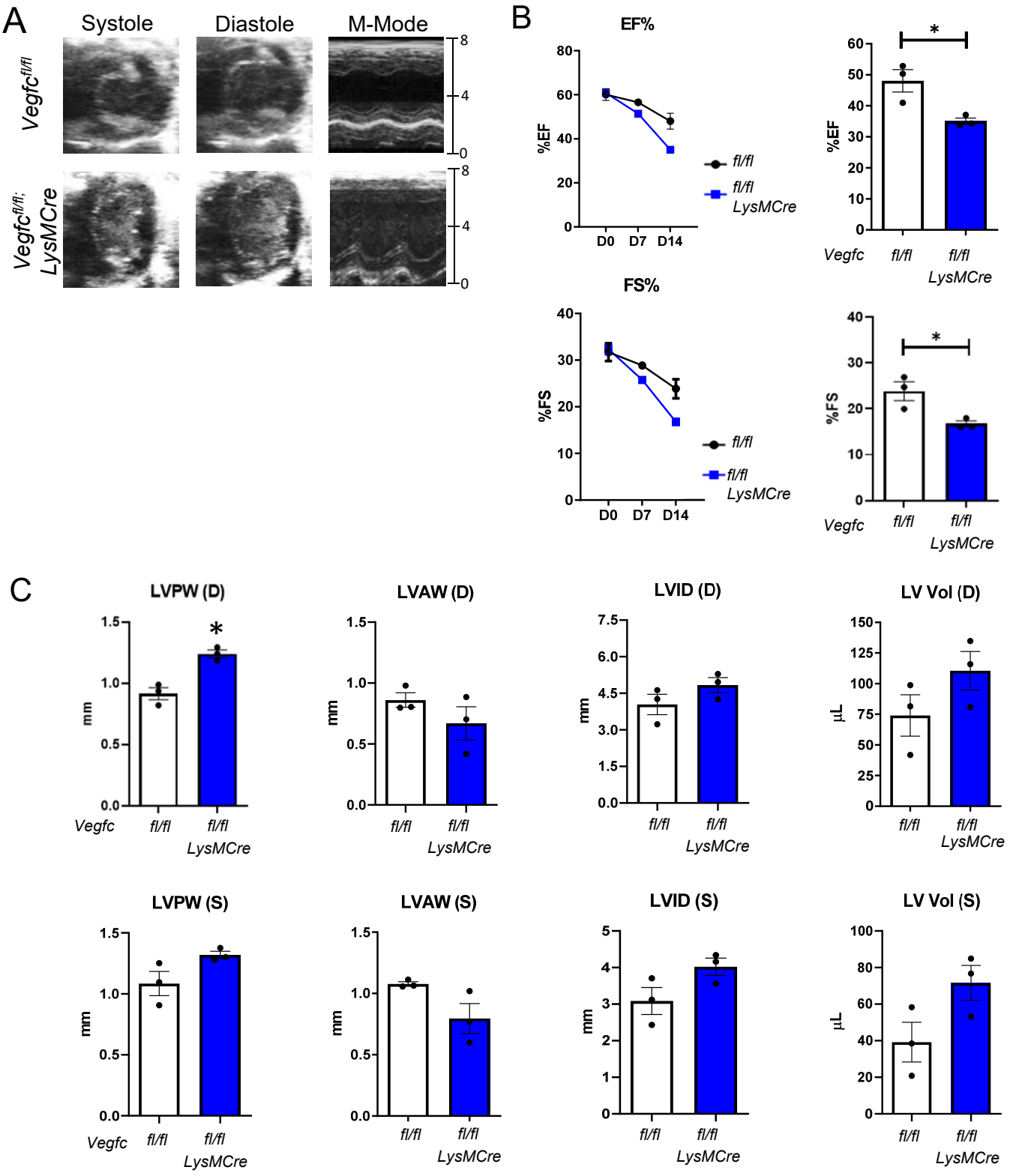

Supplemental Figure 5. Myeloid *Vegfc* deficiency leads to impaired cardiac function after reperfusion of ischemic hearts. (**A**) *Vegfc*$^{fl/fl}$*;LysMCre* mice along with littermate controls were subjected to LAD ligation followed by reperfusion (ischemia reperfusion I/R). Parasternal short-axis M-mode measurements were collected at prior to surgery (D0) and again at D14 post IRI procedure. (**B**) Time course of cardiac function between experiment groups at indicated days (D) post I/R per %EF and %FS as measurements of cardiac function. n = 3/group. * $p < 0.05$. (**C**) Parameters gained from parasternal M-mode measurements describing degree of anterior wall thinning, ventricular diameter, and volume in *Vegfc*-deficient animals after I/R. (d) Diastole, (s) Systole. n = 3/group. * $p < 0.05$.

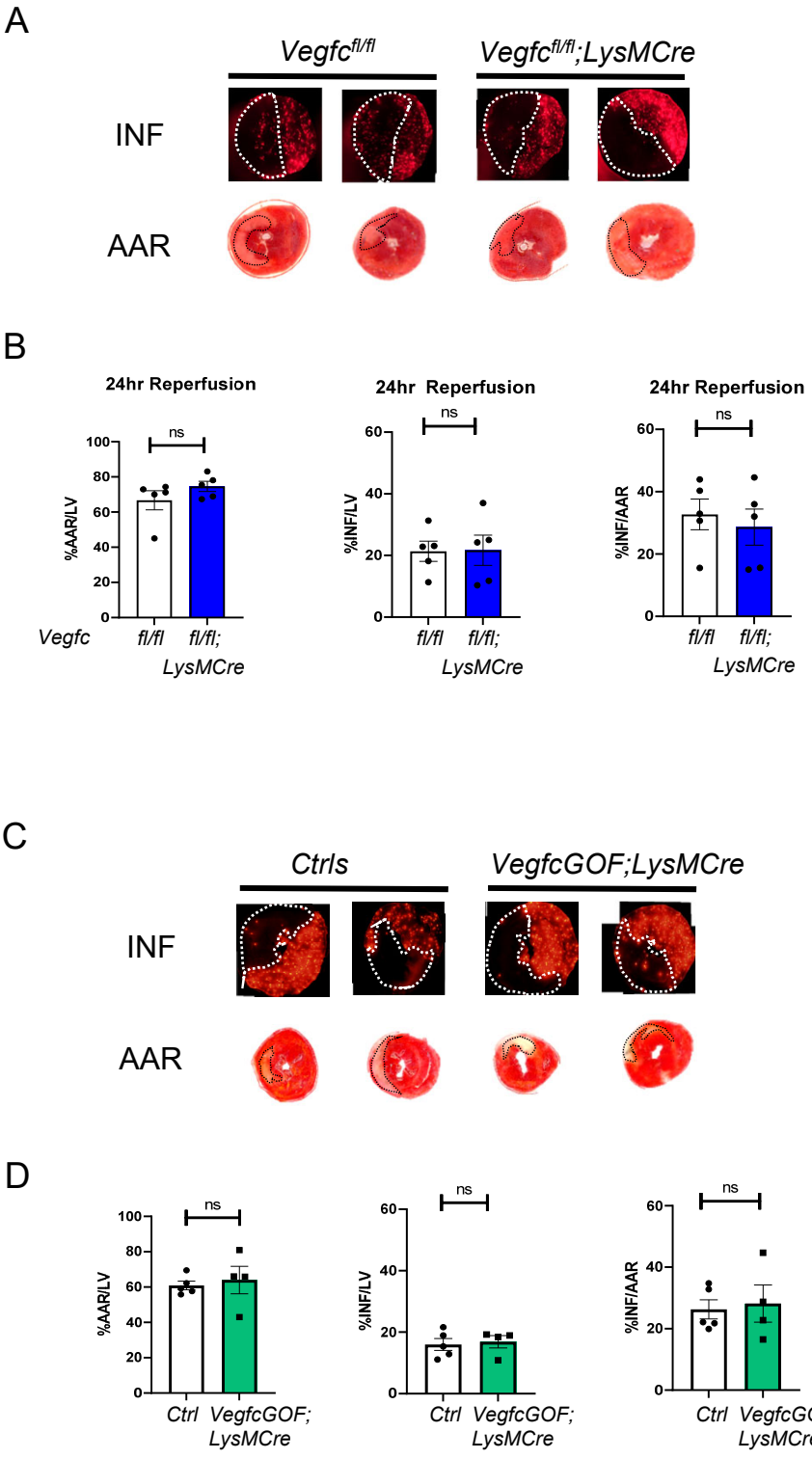

Supplemental Figure 6. Myeloid-derived VEGFC does not affect infarct size 24h post I/R. (A) *Vegfc*$^{fl/fl}$ and *Vegfc*$^{fl/fl}$*;LysMCre* mice were subjected ischemia then reperfusion (I/R). Area-at-risk (AAR) was determined by intramyocardial circulation of fluorescent microbeads, while infarct (INF) size was determined by TTC staining after 24hrs reperfusion and quantified in (**B**) n = 5 mice per group. NS – No significance **(C)** In a similar fashion, infarct and area-at-risk measurements were obtained in *VegfcGOF;LysMcre* and littermate controls and quantified in (D). N = 4-5 mice per group. No significant difference in acute injury were observed between groups.

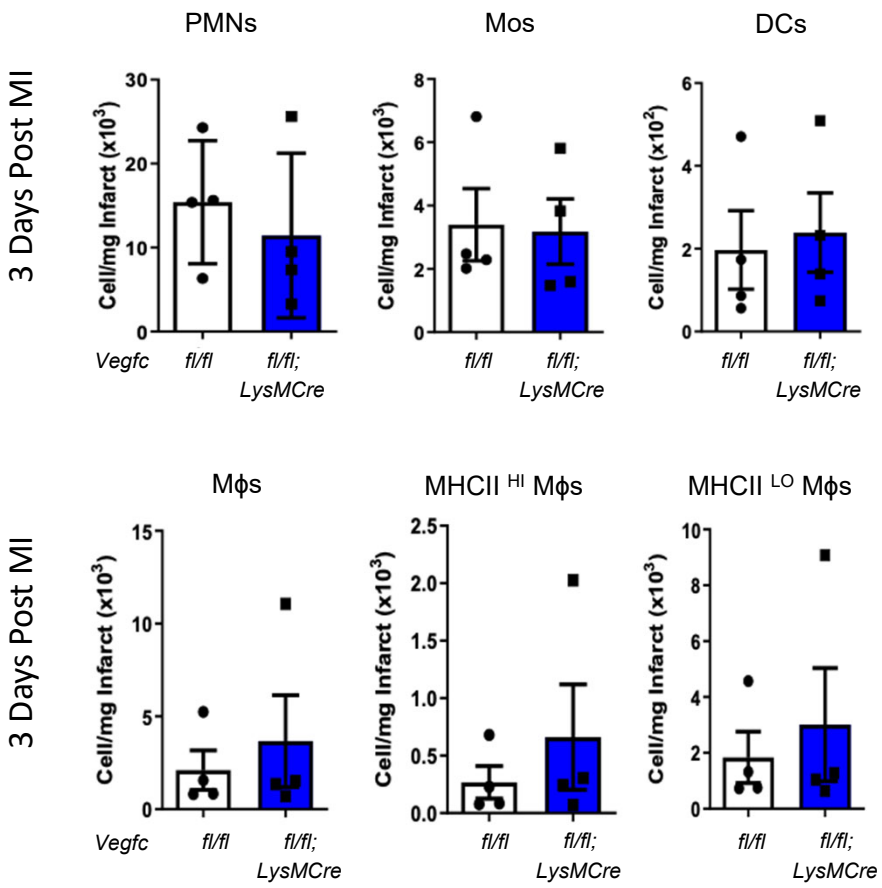

Supplemental Figure 7. Day 3 levels of inflammatory cells post MI. Flow cytometric analysis of indicated cardiac cell types at 3 days post-MI between *Vegfc*$^{fl/fl}$*;LysMCre* mice and *Vegfc*$^{fl/fl}$ littermate controls. n =4/group.

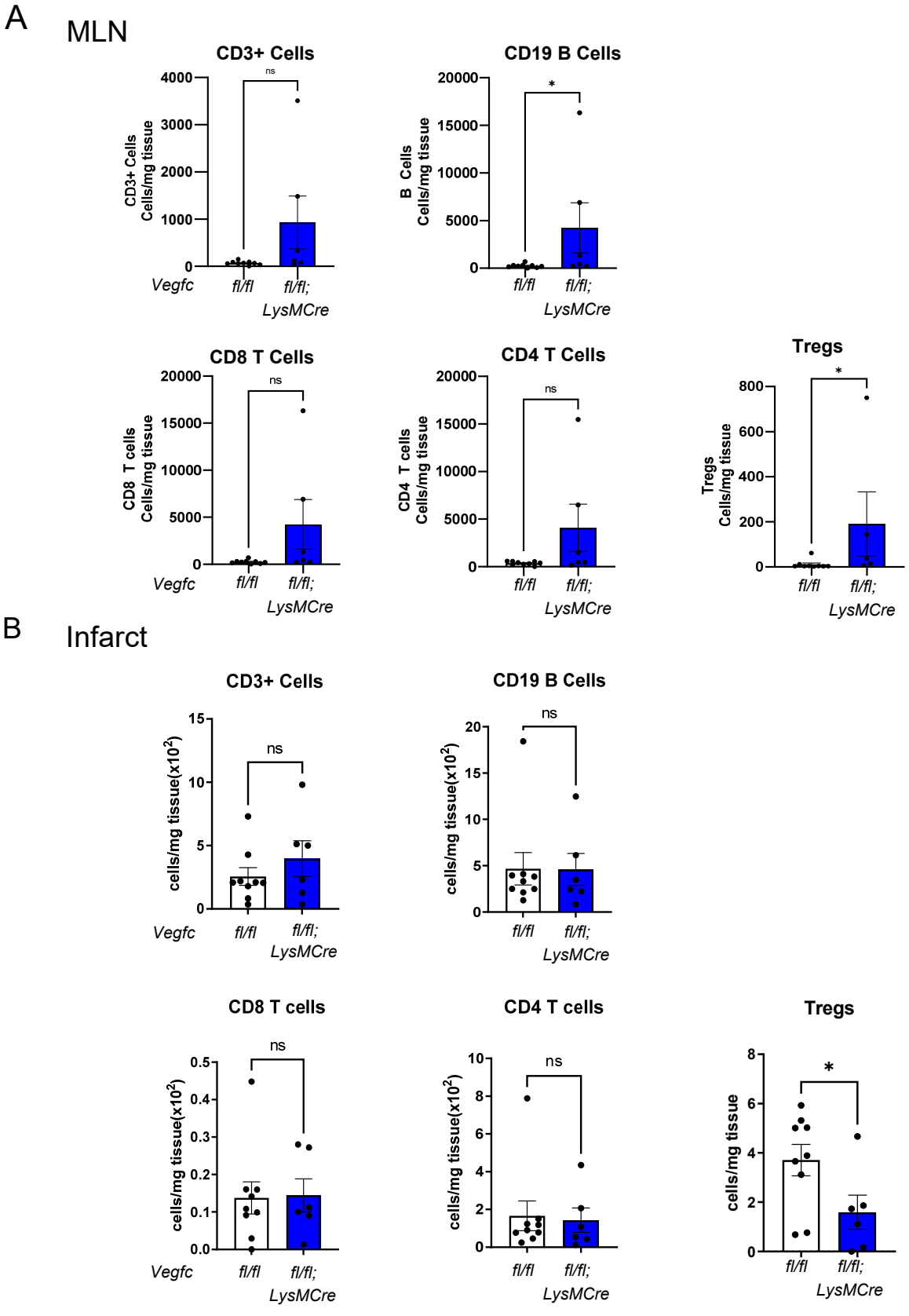

Supplemental Figure 8. Myeloid VEGFC promotes infarct associated Tregs post MI. (**A**) Flow cytometric analysis of lymphocytes in mediastinal lymph node (MLN) show higher level of B cells and Tregs in *Vegfc$^{fl/fl}$;LysMCre* mice compared to *Vegfc$^{fl/fl}$* littermate controls. (**B**) 7 days post-MI infarcts however had significantly lower Treg infiltration in *Vegfc$^{fl/fl}$;LysMCre* mice compared to littermate controls. n =6-8 per group.* $p < 0.05$ using Mann-Whitney U test.

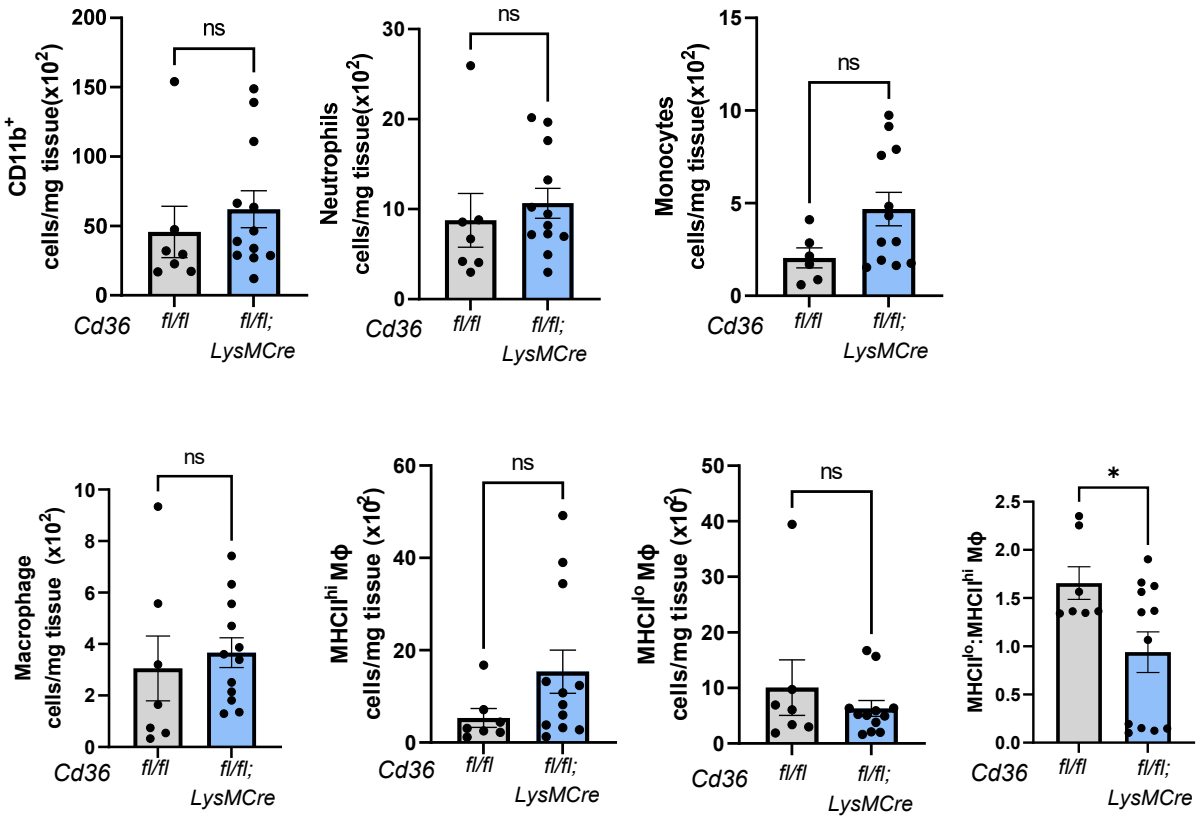

Supplemental Figure 9. Evidence for heightened cardiac and macrophage inflammation in myeloid *Cd36*-deficient mice. (**A**) Flow cytometric analysis of ischemic area at risk 7-days post MI in *Cd36* deficient mice revealed similar levels of $CD11b^{+}Ly6g^{+}$ neutrophils, $Ly6c^{hi}$ monocytes, and $CD64^{+}F4/80^{+}$ Mϕs compared to controls. Importantly, the ratio of $MHCII^{lo}$ to $MHCII^{hi}$ macrophages within the infarcted myocardium was significantly altered similarly to *Vegfc* deficient mice. * $p < 0.05$. n = 7-12 per group.

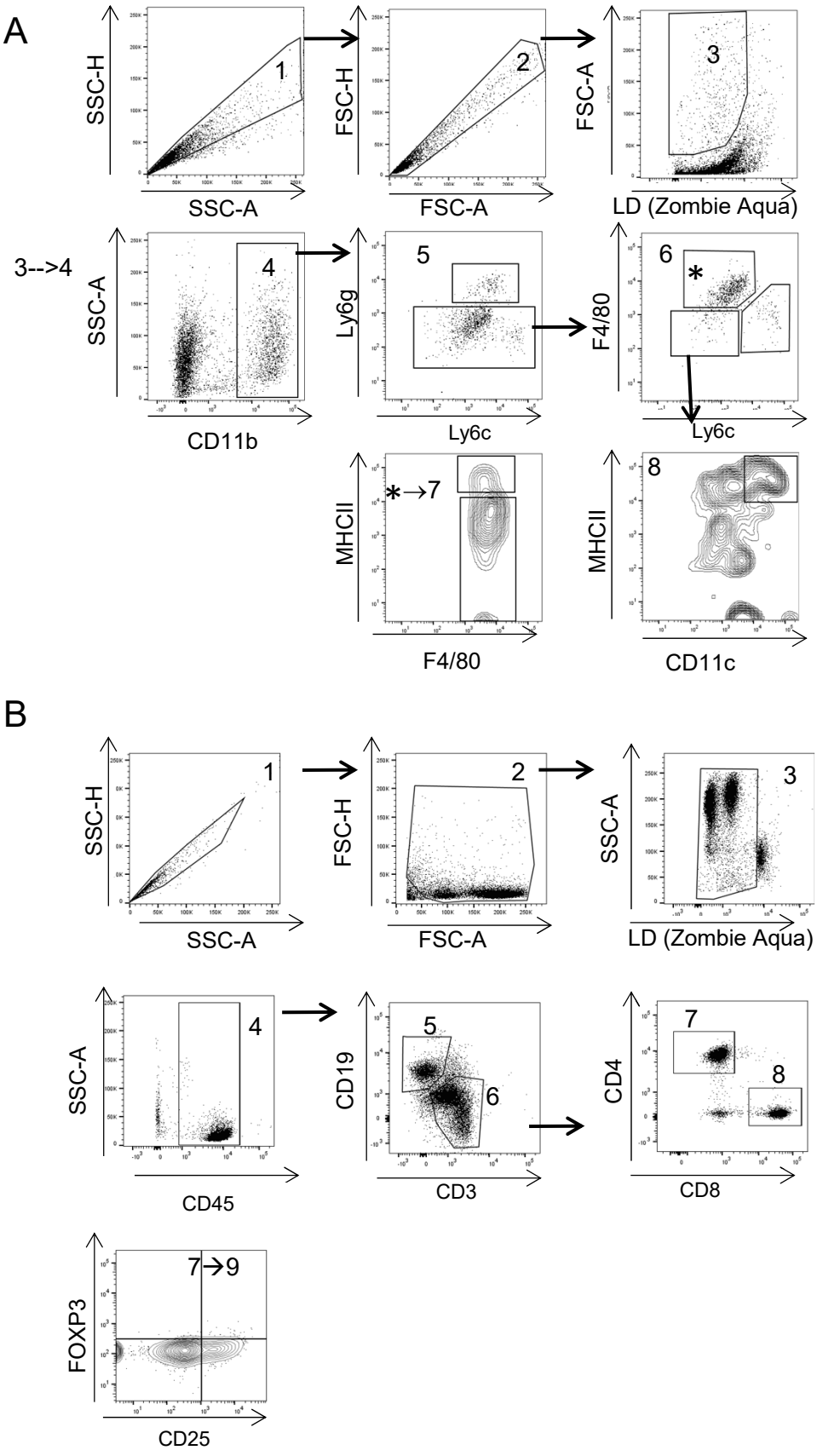

Supplemental Figure 10. Gating strategy for myeloid and lymphoid cells in mouse hearts post myocardial infarction. (**A**) Gating strategy for myeloid cells post coronary occlusion. After gating for doublets and dead cells, CD11b cells further separated by standard myeloid markers for levels of $CD11b^{+}Ly6g^{+}$ neutrophils, $CD11b^{+}Ly6G^{lo}Ly6C^{hi}F4/80^{-}$ monocytes, $CD11b^{+}MHCII^{hi}CD11c^{hi}$ DCs and $CD64^{+}F4/80^{+}$ Mϕs. (**B**) For lymphoid cells, $CD45^{+}$ cells were further separated using lymphoid markers. Cells were separated first by CD3 and CD19 expression (B cells). CD3 cells were further analyzed by CD4 and CD8 expression. Tregs were identified as $CD4^{+}CD25^{+}FOXP3^{+}$.

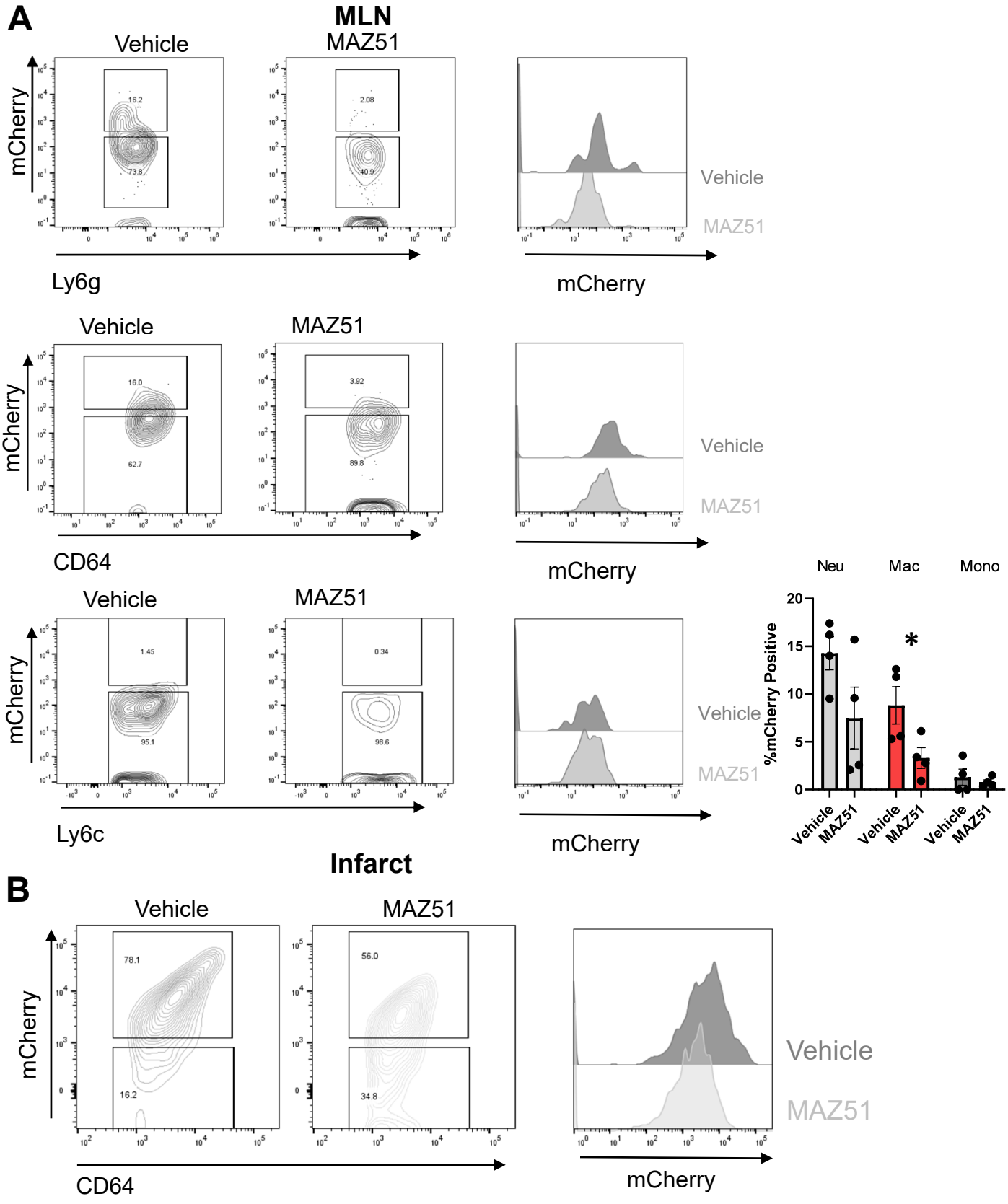

Supplemental Figure 11. mCherry antigen detected in myeloid cells post myocardial infarction is affected by VEGFR3 inhibition. (**A**) Post coronary occlusion flow cytometric analysis of medialstinal lymph nodes and relative levels of mCherry antigen uptake by Ly6g neutrophil-like cells, CD64 macrophages, and Ly6c monocyte-like cells, after treatment with VEGFR3 inhibitor MAZ51. (**B**) Flow cytometric analysis depcits decrease in mCherry antigen uptake by CD64⁺ macrophages in infarct area after treatment with MAZ51 3 days post MI.

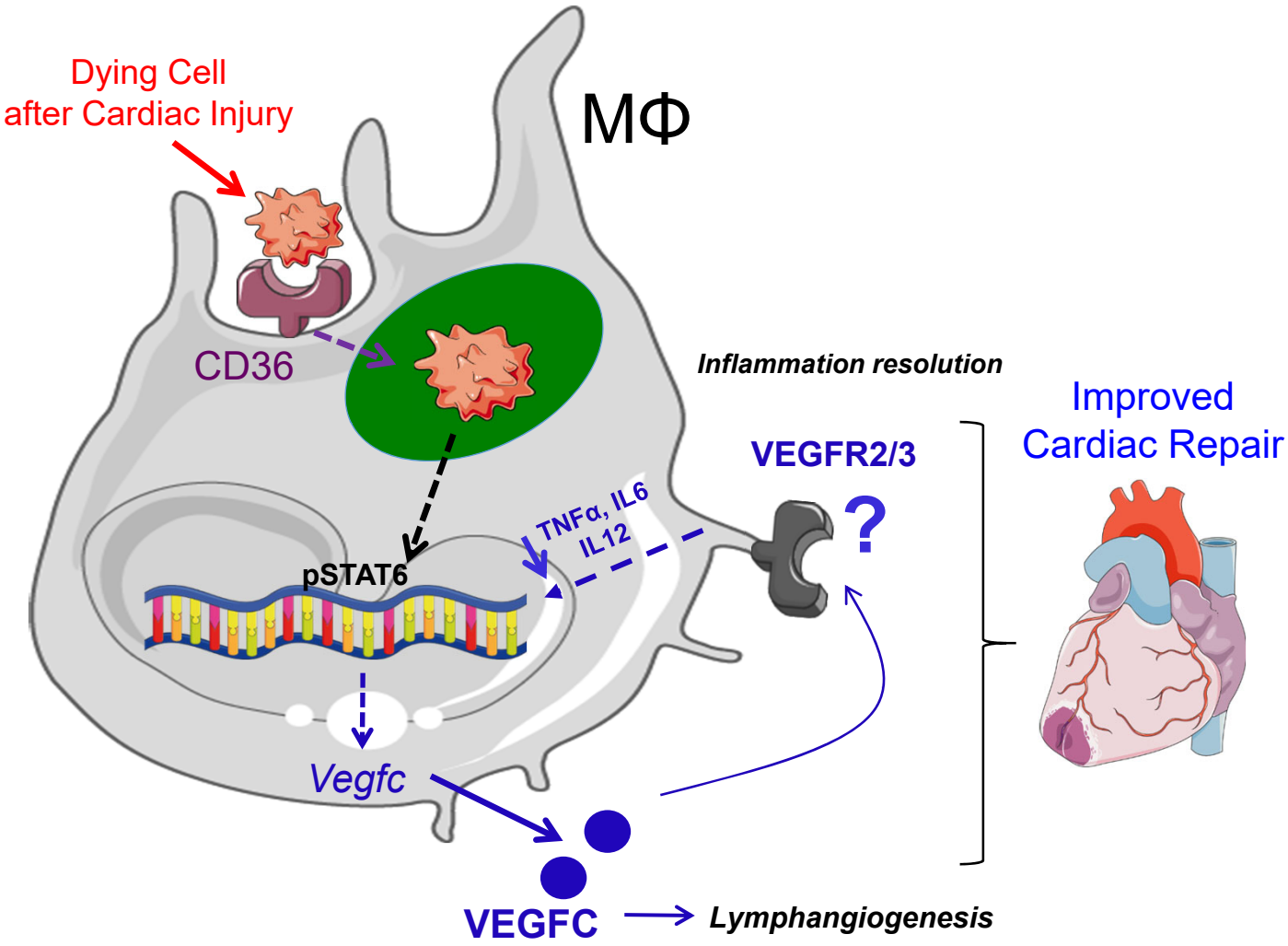

Supplemental Figure 12. Working model based on experimental findings. The schematic describes a scenario wherein cardiac damage after myocardial infarction, leads to phagocytosis of dying cells in the myocardium and the induction of macrophage VEGFC, leading to cardiac lymphangiogenesis and inflammation resolution. Macrophage = Mϕ.

Full uncut gels

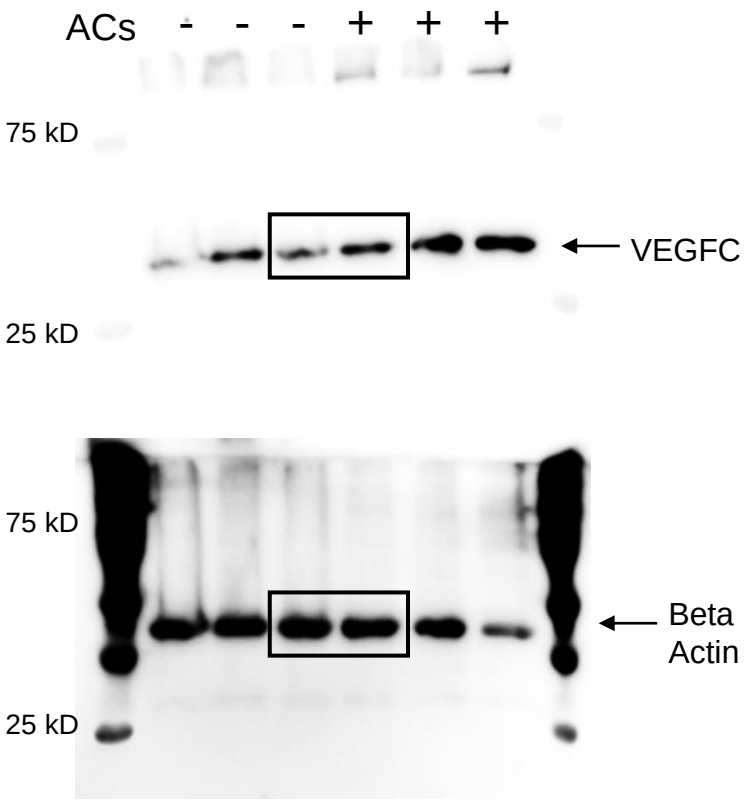

Figure 2. *Vegfc* is induced in macrophages (Mϕs) during efferocytosis. (C) Representative protein immunoblots of VEGFC 6 hours after efferocytosis and densitometry analysis.

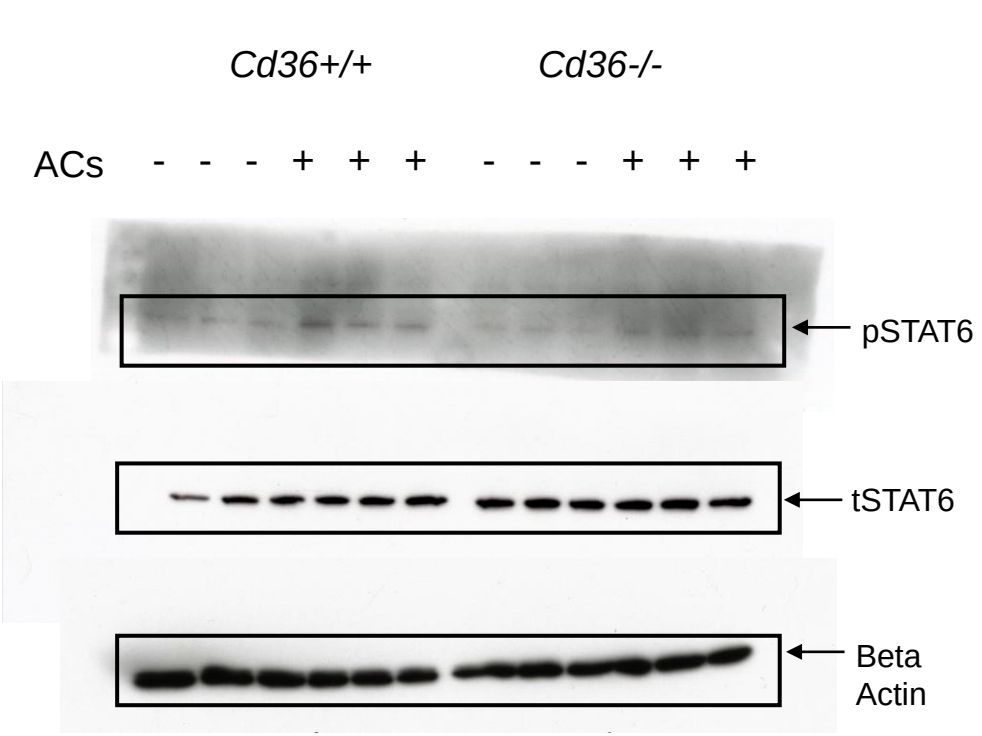

Figure 2. *Vegfc* is induced in macrophages (Mϕs) during efferocytosis. (**J**) To assess STAT6 phosphorylation Mϕs were cultured as above, and lysates were prepared in RIPA buffer then assessed by Western blotting.